JACS
JOURNAL OF THE AMERICAN CHEMICAL SOCIETY
Communication
pubs.acs.org/JACS

Perovskite $CH_3NH_3PbI_3(Cl)$ Single Crystals: Rapid Solution Growth, Unparalleled Crystalline Quality, and Low Trap Density toward 10^8 cm^{-3}

Zhipeng Lian,[†] Qingfeng Yan,*[,†] Taotao Gao,[†] Jie Ding,[†] Qianrui Lv,[†] Chuangang Ning,[‡] Qiang Li,[†] and Jia-lin Sun*[,‡]

[†]Department of Chemistry, Tsinghua University, Beijing 100084, China

[‡]Collaborative Innovation Center of Quantum Matter, State Key Laboratory of Low-Dimensional Quantum Physics, Department of Physics, Tsinghua University, Beijing 100084, China

Supporting Information

ABSTRACT: Single crystal reflects the intrinsic physical properties of a material, and single crystals with high-crystalline quality are highly desired for the acquisition of high-performance devices. We found that large single crystals of perovskite $CH_3NH_3PbI_3(Cl)$ could be grown rapidly from chlorine-containing solutions. Within 5 days, $CH_3NH_3PbI_3(Cl)$ single crystal as large as 20 mm × 18 mm × 6 mm was harvested. As a most important index to evaluate the crystalline quality, the full width at half-maximum (fwhm) in the high-resolution X-ray rocking curve (HR-XRC) of as-grown $CH_3NH_3PbI_3(Cl)$ single crystal was measured as 20 arcsec, which is far superior to so far reported $CH_3NH_3PbI_3$ single crystals (~1338 arcsec). The unparalleled crystalline quality delivered a low trap-state density of down to 7.6×10^8 cm^{-3}, high carrier mobility of 167 ± 35 cm^2 V^{-1} s^{-1}, and long transient photovoltaic carrier lifetime of 449 ± 76 μs. The improvement in the crystalline quality, together with the rapid growth rate and excellent carrier transport property, provides state-of-the-art single crystalline hybrid perovskite materials for high-performance optoelectronic devices.

Organic−inorganic hybrid perovskites such as $CH_3NH_3PbX_3$ (X = I, Br, Cl) have been deemed as strong candidates for solution processed semiconductor devices.[1] Recently, one major finding was reported that single crystal of $CH_3NH_3PbI_3$ ($MAPbI_3$) demonstrated much lower trap-state density of about 10^{10} cm^{-3} and longer carrier diffusion length (exceeding 175 μm) than those of $MAPbI_3$ polycrystalline films (~10^{15} cm^{-3} and ~100 nm, respectively).[2,3] Since then increasing attention has been attached to single-crystalline perovskites and a new generation of optoelectronic devices, such as photodetectors,[4] X-ray detectors,[5] and solar cells,[6] have been demonstrated based on single-crystalline hybrid perovskites.

High crystalline quality of a single-crystalline semiconductor material is crucial to both commercial applications and scientific investigations because it highly affects the key parameters such as trap-state density and charge transport property.[2,7] However, it is particularly challenging to obtain commercially desired single crystal materials with a combination of large size, rapid growth rate, and high crystalline quality. In order to grow large single crystals of $MAPbI_3$, great efforts have been made. Our group,[4] Tao's group,[8] and Huang's group[2] adopted solution temperature-lowering (STL) methods to grow centimeter-sized $MAPbI_3$ single crystals. However, such methods seem to be time-consuming (typically 2−4 weeks to obtain one-centimeter-sized crystals).[4,8] Subsequently, rapid inverse temperature crystallization (ITC) methods were proposed. Saidaminov and co-workers realized rapid crystal growth and prepared ~5 mm-in-length $MAPbI_3$ single crystals within only 3 h.[9] Liu et al. grew the largest $MAPbI_3$ crystal so far (two-inch in size) by using the ITC method, showing an inviting vista of commercialization.[10] Unfortunately, it was observed that single crystals grown from the ITC method suffered from solvent corrosion, leading to degenerated crystalline quality.[11,12] Furthermore, so far few studies have focused on the crystalline quality of perovskite single crystal materials as much as the growth rate and size, yet high structural perfection in $MAPbI_3$ bulk crystals is still lacking.[13] For instance, as an important index to evaluate the crystalline quality of single crystal, the full-width at half-maximum (fwhm) of X-ray diffraction rocking curve (XRC) of $MAPbI_3$ (measured as ~1338 arcsec),[10] is far inferior to some familiar semiconductor bulk crystals, such as SiC (27 arcsec),[14] AlN (72 arcsec),[15] and GaN (90 arcsec).[16]

Regarding the preparation of perovskite polycrystalline films, it was usually observed that chlorine incorporation into the precursor resulted in more continuous films of better quality.[17] Snaith and co-workers applied the mixed halide perovskite with the general formula $MAPbI_{3-x}Cl_x$ to planar heterojunction perovskite solar cells, showing high solar-to-electrical power conversion efficiency (PCE) of over 15%.[18] The mixed halide perovskite $MAPbI_{3-x}Cl_x$ was demonstrated to possess a substantially longer carrier diffusion length exceeding 1 μm.[19] Thereafter, the mixed halide perovskite $MAPbI_{3-x}Cl_x$ has attracted a huge amount of research interest and has improved PCE of solar cells up to nearly 19%.[20] Accumulative efforts pointed to the conclusion that chloride incorporation governed the morphology evolution and crystallinity in the polycrystalline perovskite absorber, therefore improving device performance.[20,21]

Received: June 9, 2016
Published: July 26, 2016

DOI: 10.1021/jacs.6b05683
J. Am. Chem. Soc. 2016, 138, 9409−9412

We were thus inspired to grow high-quality $MAPbI_3(Cl)$ large single crystals by employing chlorine to mediate the solution growth process. Benefited from the chlorine promoters, the growth rate was improved dramatically. We obtained large $MAPbI_3(Cl)$ single crystal of 20 mm × 18 mm × 6 mm within 5 days (Figure 1). Its mirror-like smooth surface was observed

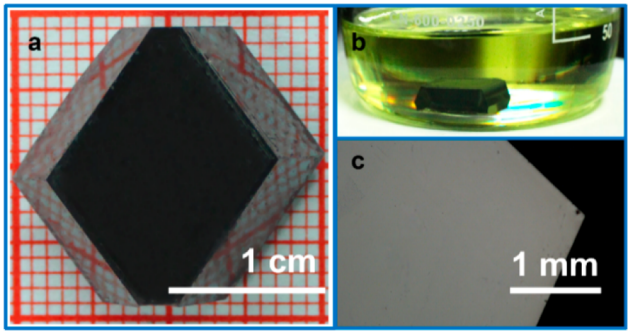

Figure 1. (a) Photograph of seed-induced-grown $MAPbI_3(Cl)$ bulk single crystal with the dimension of 20 mm × 18 mm × 6 mm. (b) Photograph of $MAPbI_3(Cl)$ bulk single crystal incubated in the solution at room temperature. (c) Microscopic image for (100) facet of as-grown $MAPbI_3(Cl)$ bulk single crystal.

under a microscope. For comparison, we also grew $MAPbI_3$ single crystals from chlorine-free systems by using aforementioned STL method (namely: bottom seeded solution growth, BSSG) and ITC method,[4,8−10] and marked them as $MAPbI_3$@STL and $MAPbI_3$@ITC, respectively (Figure S1, Supporting Information).

Rietveld structural refinement confirmed the space group *I*4/*mcm* (140) of as-grown $MAPbI_3(Cl)$ at room temperature (Figure S2, Supporting Information). The X-ray 2θ scan on the maximal (100) facet of $MAPbI_3(Cl)$ shows only (200) and (400) diffraction peaks, suggesting good single crystalline quality (Figure S3, Supporting Information). To evaluate the crystalline quality, as shown in Figure 2, we performed high-resolution XRC of the (400) diffraction and measured an unprecedented fwhm of 20 arcsec in as-grown $MAPbI_3(Cl)$, which is less than $MAPbI_3$@STL (~35 arcsec) and far better than $MAPbI_3$@ITC (~225 arcsec). It is worth emphasizing that the measured record-high

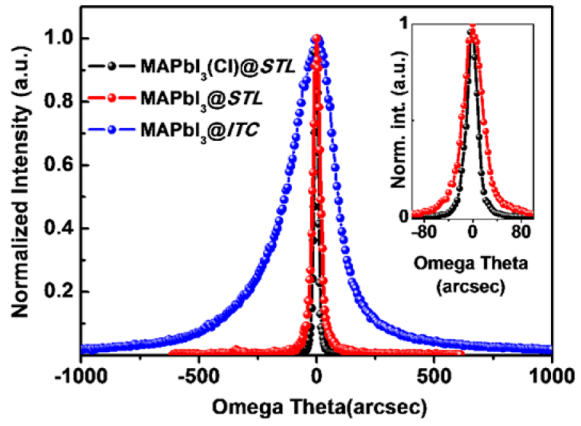

Figure 2. High-resolution X-ray diffraction rocking curves of the (400) diffraction of as-grown single crystals, which display a fwhm of ~20 arcsec for $MAPbI_3(Cl)$, ~35 arcsec for $MAPbI_3$@STL, and ~225 arcsec for $MAPbI_3$@ITC, respectively. The inset shows the detailed curves for solution-grown $MAPbI_3(Cl)$ and $MAPbI_3$@STL single crystals.

fwhm demonstrates the ultrahigh structural perfection in these as-grown $MAPbI_3(Cl)$ single crystals, which is superior to a wide array of established inorganic single crystalline semiconductors.[14−16]

To investigate the trap-state density n_{trap} and estimate the carrier mobility μ ($\mu = \mu_p \approx \mu_n$, where μ_p and μ_n are the hole and electron mobility, respectively) of as-grown $MAPbI_3(Cl)$ single crystals, we measured the dark current−voltage (I−V) traces according to the space charge-limited current (SCLC) model (Figure 3).[2,7] With the increasing bias voltage, the current I

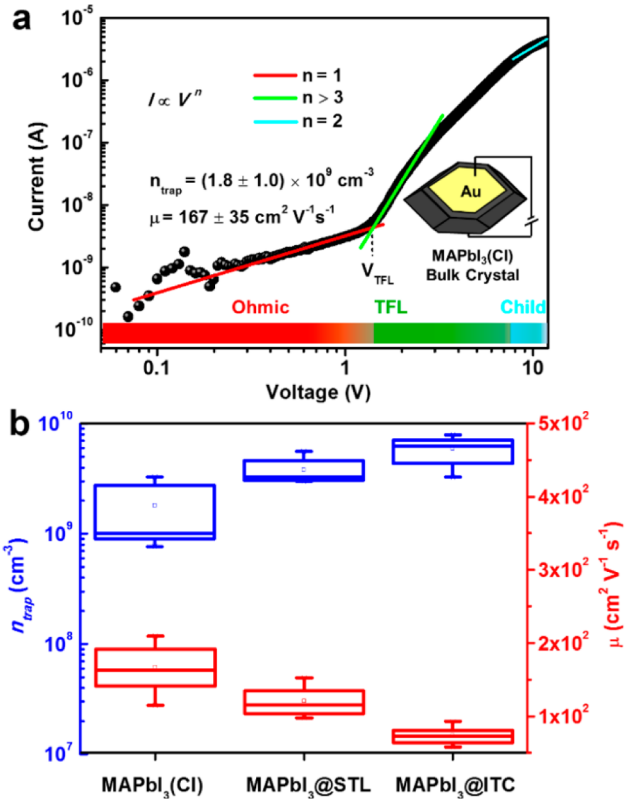

Figure 3. Dark current−voltage measurements according to the space charge-limited current (SCLC) model. (a) I−V trace of $MAPbI_3(Cl)$ single crystal exhibiting three different regimes, marked for Ohmic ($I \propto V^{n=1}$), trap-filled ($I \propto V^{n>3}$), and Child's ($I \propto V^{n=2}$) regime. (b) Calculated trap-state densities (blue) and charge carrier transport mobilities (red) for $MAPbI_3(Cl)$, $MAPbI_3$@STL, and $MAPbI_3$@ITC, respectively.

increased from the linear Ohmic region, through a trap-filled limit (V_{TFL}), then eventually to the quadratic Child's region, as shown in Figure 3a. $MAPbI_3(Cl)$ single crystals exhibit a higher carrier mobility of 167 ± 35 $cm^2\ V^{-1}\ s^{-1}$ and much lower trap-state density of (1.80 ± 1.07) × 10^9 cm^{-3}, followed by $MAPbI_3$@STL (121 ± 20 $cm^2\ V^{-1}\ s^{-1}$ and (3.82 ± 1.06) × 10^9 cm^{-3}) and then $MAPbI_3$@ITC (74 ± 12 $cm^2\ V^{-1}\ s^{-1}$ and (5.95 ± 1.77) × 10^9 cm^{-3}), where the uncertainty represents the standard deviation. Consistent with the high-resolution XRC measurement results, the $MAPbI_3(Cl)$ single crystals demonstrate fewer trap states. It is thus deduced that the improvement on crystalline perfection improves the charge carrier transport property. Note that the significantly reduced trap-state density in as-grown high crystalline quality $MAPbI_3(Cl)$ (~10^9 cm^{-3} in average and with the best of 7.6 × 10^8 cm^{-3}) is an order of magnitude lower than

DOI: 10.1021/jacs.6b05683
J. Am. Chem. Soc. 2016, 138, 9409−9412

that in previously reported $MAPbI_3$ single crystals ($\sim 10^{10}$ cm^{-3}).[2,7,9]

The recombination lifetime of as-grown single crystals was then characterized with transient photovoltaic (TPV) method. At 0.1 sun illumination (532 nm, 10 mW cm^{-2}), the TPV lifetime for $MAPbI_3(Cl)$ single crystal was measured as 449 ± 76 μs (Figure 4). Improvement on crystalline quality reduced the

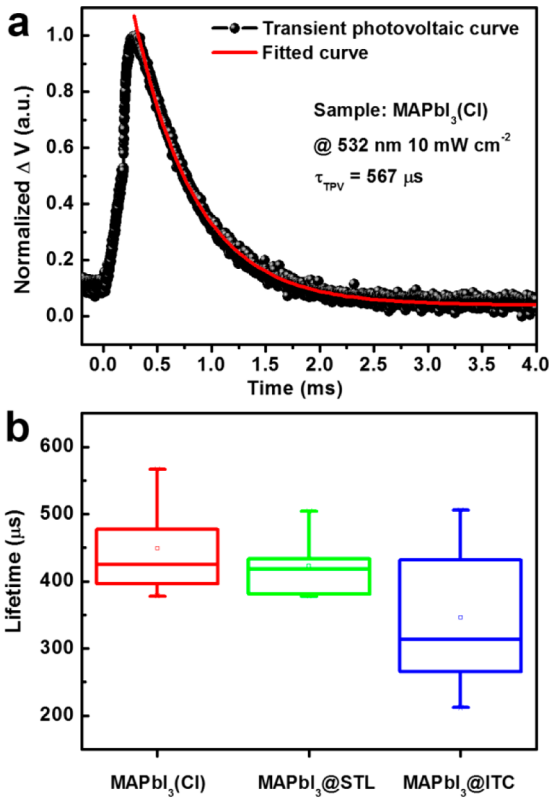

Figure 4. Transient photovoltaic (TPV) measurements. (a) TPV lifetime for $MAPbI_3(Cl)$ single crystal. (b) Lifetimes of $MAPbI_3(Cl)$, $MAPbI_3$@STL, and $MAPbI_3$@ITC based on TPV measurements.

charge carrier recombination, thus leading to the extension of carrier lifetimes in $MAPbI_3(Cl)$ bulk crystals. It should be also noted that the lifetime measured by TPV method is strongly dependent on the light intensity and the long lifetime might be caused by the so-called photon recycling effect in the bulk single crystals.[2,22]

Chlorine incorporation improved the crystalline quality in $MAPbI_3(Cl)$ single crystals. However, the presence and effect of the incoming chlorine need to be identified. Indeed, until today, the role of extrinsic chlorine incorporation has not yet been fully understood, and the presence of chlorine in so-called $MAPbI_{3-x}Cl_x$ has been long debated.[20] A variety of technologies have been used to determine the existence of chlorine in $MAPbI_{3-x}Cl_x$ films.[20,23,24] All these previous studies were normally based on $MAPbI_{3-x}Cl_x$ polycrystalline films. In these cases characterizations might be affected by the presence of residual impurity phases from the precursor solutions. Here we attempt to ascertain the presence of chlorine in $MAPbI_3$ crystal textures by utilizing as-grown $MAPbI_3(Cl)$ single crystal as a platform. X-ray photoelectron spectroscopy (XPS) spectra scan from the top surface, and depth profile showed no trace of Cl appearing in the $MAPbI_3(Cl)$ single crystal (Figure S4, Supporting Information). Considering the detecting limit of XPS, we carried out time-of-flight secondary ion mass spectroscopy (ToF-SIMS) depth profiling (Figure 5). The result clearly

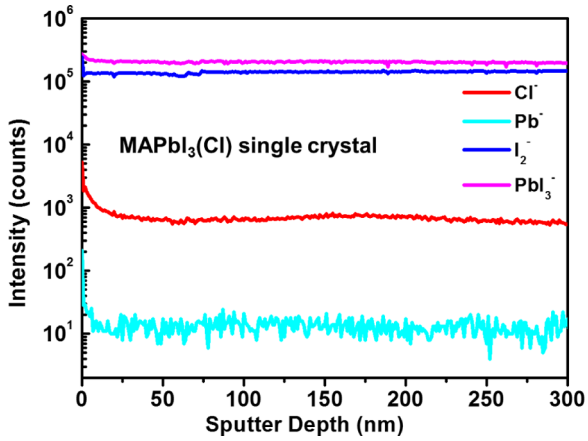

Figure 5. Depth profiling of time-of-flight secondary ion mass spectroscopy (ToF-SIMS) for $MAPbI_3(Cl)$ single crystal.

confirms that trace amount of chlorine went into the $MAPbI_3(Cl)$ single crystals, which is below the detecting limit of XPS. However, for the lack of a standard reference sample with known chlorine content, it is temporarily hard to determine the exact chlorine content in our $MAPbI_3(Cl)$ single crystals by ToF-SIMS method.

We observed a reduction in $MAPbI_3$ solubility with the addition of chlorine (see S7 in Supporting Information), showing a bigger drive force of phase change from solution to solid, thus leading to a rapid growth rate. In fact, with the addition of chlorine, the growth kinetics for all types of faces in the growth form of $MAPbI_3$ crystal will be affected. According to the periodic bond chains (PBC) theory by Hertman,[25] F faces of a growing crystal are smooth on a molecular level with pretty low kink densities. Because kinks are necessary for the attachment of incoming growth species, crystal growth on F faces is normally hampered unless kinks are produced, which can be accomplished by either formation of dislocations from the crystal matrix or generation of some two-dimensional (2D) nuclei on the growth layer.[25,26] Therefore, a possible growth mechanism is proposed for the rapid growth of high-quality $MAPbI_3(Cl)$ single crystals as shown in Figure 6 (see S7 for details in Supporting Information). We speculate that the role of chlorine is to provide interim kinks by forming chlorinated intermediate molecules reversibly and rapidly on the growth surface. Hence the dislocation defect density in $MAPbI_3(Cl)$ single crystal was largely reduced.

In conclusion, we report on the ultrahigh crystalline quality in $MAPbI_3(Cl)$ single crystals grown via a rapid solution temperature-lowering method. Chlorine additive effectively shortened the growth period from weeks to days and thus reduced the fabrication cost. Most importantly, it enabled the $MAPbI_3(Cl)$ single crystals to exhibit the combination of high structural perfection, low trap-state density, large size, and excellent charge transport properties at the same time. These findings indicate $MAPbI_3(Cl)$ single crystals outperform the $MAPbI_3$ single crystals reported in the literature, demonstrating the superiority of this newly developed perovskite single crystal and providing a promising material choice for the fabrication of high-performance optoelectronic devices.

DOI: 10.1021/jacs.6b05683
J. Am. Chem. Soc. 2016, 138, 9409−9412

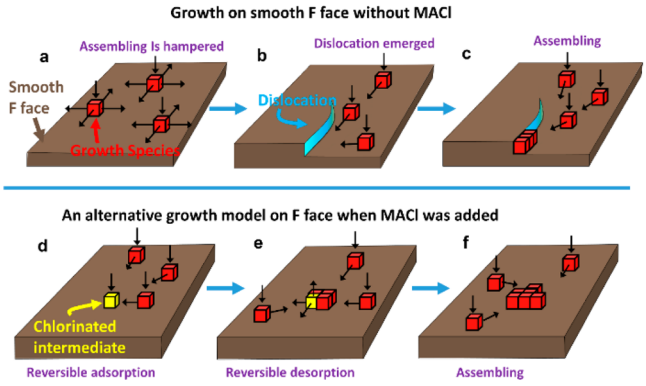

Figure 6. Schematic of crystal growth process on F face. (a–c) Growth process assisted by dislocation (blue). (a) Crystal growth on smooth F faces is normally hampered. (b) Dislocations from the crystal matrix provide sites that attract the incoming growth species (iodinated molecules, red). (c) Assembling of growth species on dislocations. (d–f) An alternative growth model showing the impact of chlorinated molecule intermediate (yellow) on crystal growth process. (d) Temporary adsorption of chlorinated molecules intermediate on the surface of a growing crystal, leading to interim kinks (2D nuclei), which attract the growth species. (e) Along with the assembling of growth species, the migration and desorption of chlorinated molecules occurred as a result of the reversible chlorinated intermediate reactions. (f) Previously assembled growth species provide kinks for further growth.

■ ASSOCIATED CONTENT

Supporting Information

The Supporting Information is available free of charge on the ACS Publications website at DOI: 10.1021/jacs.6b05683.

Full experimental details and additional spectra and characterizations (PDF)

■ AUTHOR INFORMATION

Corresponding Authors

*yanqf@mail.tsinghua.edu.cn

*jlsun@tsinghua.edu.cn

Notes

The authors declare no competing financial interest.

■ ACKNOWLEDGMENTS

The authors would like to thank the financial support from the National Science Foundation of China (Nos. 51173097, 91333109, and 11174172) and the National Key Basic Research Program of China (No. 2013CB632900). The Tsinghua University Initiative Scientific Research Program (Nos. 20131089202, 20161080165) and the Open Research Fund Program of the State Key Laboratory of Low-Dimensional Quantum Physics (No. KF201516) are also acknowledged for partial financial support.

■ REFERENCES

(1) Chueh, C.-C.; Li, C.-Z.; Jen, A. K.-Y. *Energy Environ. Sci.* **2015**, *8*, 1160.

(2) Dong, Q.; Fang, Y.; Shao, Y.; Mulligan, P.; Qiu, J.; Cao, L.; Huang, J. *Science* **2015**, *347*, 967.

(3) Xing, G.; Mathews, N.; Sun, S.; Lim, S. S.; Lam, Y. M.; Grätzel, M.; Mhaisalkar, S.; Sum, T. C. *Science* **2013**, *342*, 344.

(4) Lian, Z.; Yan, Q.; Lv, Q.; Wang, Y.; Liu, L.; Zhang, L.; Pan, S.; Li, Q.; Wang, L.; Sun, J.-L. *Sci. Rep.* **2015**, *5*, 16563.

(5) Wei, H.; Fang, Y.; Mulligan, P.; Chuirazzi, W.; Fang, H.-H.; Wang, C.; Ecker, B. R.; Gao, Y.; Loi, M. A.; Cao, L. *Nat. Photonics* **2016**, *10*, 333.

(6) Peng, W.; Wang, L.; Murali, B.; Ho, K. T.; Bera, A.; Cho, N.; Kang, C. F.; Burlakov, V. M.; Pan, J.; Sinatra, L. *Adv. Mater.* **2016**, *28*, 3383.

(7) Shi, D.; Adinolfi, V.; Comin, R.; Yuan, M.; Alarousu, E.; Buin, A.; Chen, Y.; Hoogland, S.; Rothenberger, A.; Katsiev, K. *Science* **2015**, *347*, 519.

(8) Dang, Y.; Liu, Y.; Sun, Y.; Yuan, D.; Liu, X.; Lu, W.; Liu, G.; Xia, H.; Tao, X. *CrystEngComm* **2015**, *17*, 665.

(9) Saidaminov, M. I.; Abdelhady, A. L.; Murali, B.; Alarousu, E.; Burlakov, V. M.; Peng, W.; Dursun, I.; Wang, L.; He, Y.; Maculan, G. *Nat. Commun.* **2015**, *6*, 7586.

(10) Liu, Y.; Yang, Z.; Cui, D.; Ren, X.; Sun, J.; Liu, X.; Zhang, J.; Wei, Q.; Fan, H.; Yu, F. *Adv. Mater.* **2015**, *27*, 5176.

(11) Rong, Y.; Tang, Z.; Zhao, Y.; Zhong, X.; Venkatesan, S.; Graham, H.; Patton, M.; Jing, Y.; Guloy, A. M.; Yao, Y. *Nanoscale* **2015**, *7*, 10595.

(12) Hao, F.; Stoumpos, C. C.; Liu, Z.; Chang, R. P.; Kanatzidis, M. G. *J. Am. Chem. Soc.* **2014**, *136*, 16411.

(13) Dang, Y.; Ju, D.; Wang, L.; Tao, X. *CrystEngComm* **2016**, *18*, 4476.

(14) Nakamura, D.; Gunjishima, I.; Yamaguchi, S.; Ito, T.; Okamoto, A.; Kondo, H.; Onda, S.; Takatori, K. *Nature* **2004**, *430*, 1009.

(15) Sumathi, R. R. *CrystEngComm* **2013**, *15*, 2232.

(16) Hashimoto, T.; Wu, F.; Speck, J. S.; Nakamura, S. *Nat. Mater.* **2007**, *6*, 568.

(17) Yang, B.; Keum, J.; Ovchinnikova, O. S.; Belianinov, A.; Chen, S.; Du, M.-H.; Ivanov, I. N.; Rouleau, C. M.; Geohegan, D. B.; Xiao, K. *J. Am. Chem. Soc.* **2016**, *138*, 5028.

(18) Liu, M.; Johnston, M. B.; Snaith, H. J. *Nature* **2013**, *501*, 395.

(19) Stranks, S. D.; Eperon, G. E.; Grancini, G.; Menelaou, C.; Alcocer, M. J.; Leijtens, T.; Herz, L. M.; Petrozza, A.; Snaith, H. J. *Science* **2013**, *342*, 341.

(20) Chae, J.; Dong, Q.; Huang, J.; Centrone, A. *Nano Lett.* **2015**, *15*, 8114.

(21) Chen, Q.; Zhou, H.; Fang, Y.; Stieg, A. Z.; Song, T.-B.; Wang, H.-H.; Xu, X.; Liu, Y.; Lu, S.; You, J. *Nat. Commun.* **2015**, *6*, 7269.

(22) Pazos-Outón, L. M.; Szumilo, M.; Lamboll, R.; Richter, J. M.; Crespo-Quesada, M.; Abdi-Jalebi, M.; Beeson, H. J.; Vrućinić, M.; Alsari, M.; Snaith, H. J. *Science* **2016**, *351*, 1430.

(23) Yu, H.; Wang, F.; Xie, F.; Li, W.; Chen, J.; Zhao, N. *Adv. Funct. Mater.* **2014**, *24*, 7102–7108.

(24) Unger, E. L.; Bowring, A. R.; Tassone, C. J.; Pool, V. L.; Gold-Parker, A.; Cheacharoen, R.; Stone, K. H.; Hoke, E. T.; Toney, M. F.; McGehee, M. D. *Chem. Mater.* **2014**, *26*, 7158.

(25) Hartman, P.; Perdok, W. *Acta Crystallogr.* **1955**, *8*, 49.

(26) Sangwal, K. *J. Cryst. Growth* **1999**, *203*, 197.

DOI: 10.1021/jacs.6b05683
J. Am. Chem. Soc. 2016, 138, 9409–9412